Developmental Biology 360 (2011) 276–285

Contents lists available at SciVerse ScienceDirect

Developmental Biology

journal homepage: www.elsevier.com/developmentalbiology

Visualizing digestive organ morphology and function using differential fatty acid metabolism in live zebrafish

Juliana Debrito Carten [a,b], Mary Katherine Bradford [a], Steven Arthur Farber [b,*]

[a] The Johns Hopkins University, Department of Biology, 3400 North Charles Street, Baltimore, MD 21218, USA
[b] The Carnegie Institution for Science, Department of Embryology, 3520 San Martin Drive, Baltimore, MD 21218, USA

ARTICLE INFO

Article history:
Received for publication 29 July 2011
Revised 13 September 2011
Accepted 13 September 2011
Available online 21 September 2011

Keywords:
Fatty acid
Metabolism
Zebrafish
BODIPY-FL
Intestine
Liver

ABSTRACT

Lipids are essential for cellular function as sources of fuel, critical signaling molecules and membrane components. Deficiencies in lipid processing and transport underlie many metabolic diseases. To better understand metabolic function as it relates to disease etiology, a whole animal approach is advantageous, one in which multiple organs and cell types can be assessed simultaneously *in vivo*. Towards this end, we have developed an assay to visualize fatty acid (FA) metabolism in larval zebrafish (*Danio rerio*). The method utilizes egg yolk liposomes to deliver different chain length FA analogs (BODIPY-FL) to six day-old larvae. Following liposome incubation, larvae accumulate the analogs throughout their digestive organs, providing a comprehensive readout of organ structure and physiology. Using this assay we have observed that different chain length FAs are differentially transported and metabolized by the larval digestive system. We show that this assay can also reveal structural and metabolic defects in digestive mutants. Because this labeling technique can be used to investigate digestive organ morphology and function, we foresee its application in diverse studies of organ development and physiology.

© 2011 Elsevier Inc. All rights reserved.

Introduction

To understand complex physiological events there is a pressing need to overlay metabolic information onto well-characterized cellular processes (McKnight, 2010). Across diverse fields, biologists routinely identify and characterize mutants using morphological criteria to uncover mechanisms underlying cellular phenomena (Morgan, 1932; Nusslein-Volhard, 1994). Techniques such as immunohistochemistry, *in situ* hybridization, and electron microscopy are utilized to visualize cellular and subcellular structure; however, these methods do not always reveal the physiological consequences of a mutation or given experimental perturbation. Furthermore, mutants lacking overt morphological abnormalities may have deficiencies in other respects (*e.g.*, behavioral or metabolic). Thus, physiological assays should also be used to screen for and functionally characterize mutants to provide a more complete understanding of gene function.

Fluorescent lipid analogs offer a way to assess both the morphology and metabolic function of digestive organs and lipid storing tissues (Farber et al., 2001). Many of the properties that make imaging lipids at the subcellular level difficult, such as their small size, dynamic subcellular behavior, and propensity to be metabolized into different species, enable lipid analogs to provide a wealth of information about a mutation's physiological impact. Advancements in lipid analogs and live-imaging techniques have improved the imaging of lipids at the subcellular level (Schultz et al., 2010), yet cultured cells remain the predominant models of choice (Guo et al., 2008; Spandl et al., 2009). To image lipid metabolism in an intact vertebrate digestive system, we have developed a feeding assay to visualize FA uptake, accumulation, and transport in live zebrafish larvae. Zebrafish possess many of the same digestive organs, cells, and genes as humans do (Andre et al., 2000; Marza et al., 2005; Schlegel and Stainier, 2006; Wallace and Pack, 2003; Wallace et al., 2005), and are currently being used as models of metabolic disorders such as diet-induced obesity (Oka et al., 2010), atherosclerosis (Stoletov et al., 2009), and diabetes (Elo et al., 2007). At the onset of exogenous feeding at approximately 5 days post-fertilization (dpf), zebrafish larvae possess a functional digestive system and remain largely transparent, allowing them to be utilized for studies of digestive physiology *in vivo* (Farber et al., 2001).

The dietary fat consumed by humans and zebrafish alike consists primarily of triacylglycerol (TAG), which must be processed by digestive enzymes and bile for intestinal absorption (Benzonana and Desnuelle, 1965; Black, 2007; Sarda and Desnuelle, 1958; Young and Hui, 1999). Pancreatic acinar cells produce, package, and secrete digestive enzymes into the pancreatic ducts by fusion of zymogen granules with the apical acinar cell membrane (reviewed by Lowe, 2002). After draining into the common bile duct, pancreatic lipases mix with bile derived from the liver. Hepatocytes drain bile into 'little canals' termed canaliculi, which direct bile into hepatic ducts that empty into the gall bladder (Lorent et al., 2004; Pack et al., 1996). In response to stimulation by the hormone cholecystokinin (CCK), bile and fat-splitting enzymes in the gall bladder are pumped into the intestinal lumen to emulsify TAG by forming mixed micelles (reviewed by Iqbal and Hussain, 2009).

* Corresponding author.
E-mail addresses: carten@ciwemb.edu (J.D. Carten), farber@ciwemb.edu (S.A. Farber)

0012-1606/$ – see front matter © 2011 Elsevier Inc. All rights reserved.
doi:10.1016/j.ydbio.2011.09.010

Free FAs and monoacylglycerols are then taken up by the absorptive cells of the intestine (Thomson et al., 1993).

Following intestinal absorption and conversion of FAs into acyl-CoA by acyl-CoA synthetases (Lehner and Kuksis, 1995; Manganaro and Kuksis, 1985a; Manganaro and Kuksis, 1985b), activated FAs have a number of potential metabolic fates including being burned to generate acetyl-CoA via alpha or beta-oxidation, synthesized into neutral lipids and stored in cytoplasmic lipid drops (Fig. 1B), or used for membrane phospholipid synthesis (Ellis et al., 2010). Neutral lipids destined for delivery to other tissues and organs in the body are secreted as intestinal lipoproteins, termed chylomicrons, from the basolateral surface of enterocytes (Fig. 1B). Following secretion, these lipoproteins travel to the liver where they bind lipoprotein receptors that are internalized and subsequently metabolized (Bloom et al., 1950; McDonald et al., 1980; Vallot et al., 1985).

In an attempt to visualize these steps of dietary FA metabolism in the digestive system of larval zebrafish, we selected BODIPY-FL analogs (Invitrogen, Inc), which have been used to visualize lipid droplets in cultured cells (Huang et al., 2004; Karsenty et al., 2009) and whole organisms (Furlong et al., 1995; Mak et al., 2006; Zhang et al., 2010). These analogs consist of a BODIPY-tagged saturated acyl chain of varying lengths. Saturated FAs are classified by their chain length (short: 2–6 carbons, medium: 8–12 carbons, long: 14–20, and very long: ≥22) (reviewed by Papamandjaris et al., 1998). The BODIPY fluorophore itself (4,4-difluoro-4-bora-3a, 4a-diaza-S-indacene) possesses several characteristics that make it useful for imaging lipids, including high photostability, a strong and narrow wavelength emission in the visible spectrum, and an overall uncharged state (Treibs and Kreuzer, 1969).

Using these fluorescent FAs we have conducted a comparative study of short, medium, and long chain FA (LCFA) BODIPY analogs. We have found that larval ingestion of different chain length analogs results in unique patterns of FA localization across multiple organs and cell types including intestinal enterocytes, hepatocytes, and pancreatic acinar cells. TLC analysis of total larval lipids confirms that the FA analogs are metabolized, with the metabolic profile of each analog consistent with its *in vivo* localization pattern. Furthermore, we have utilized

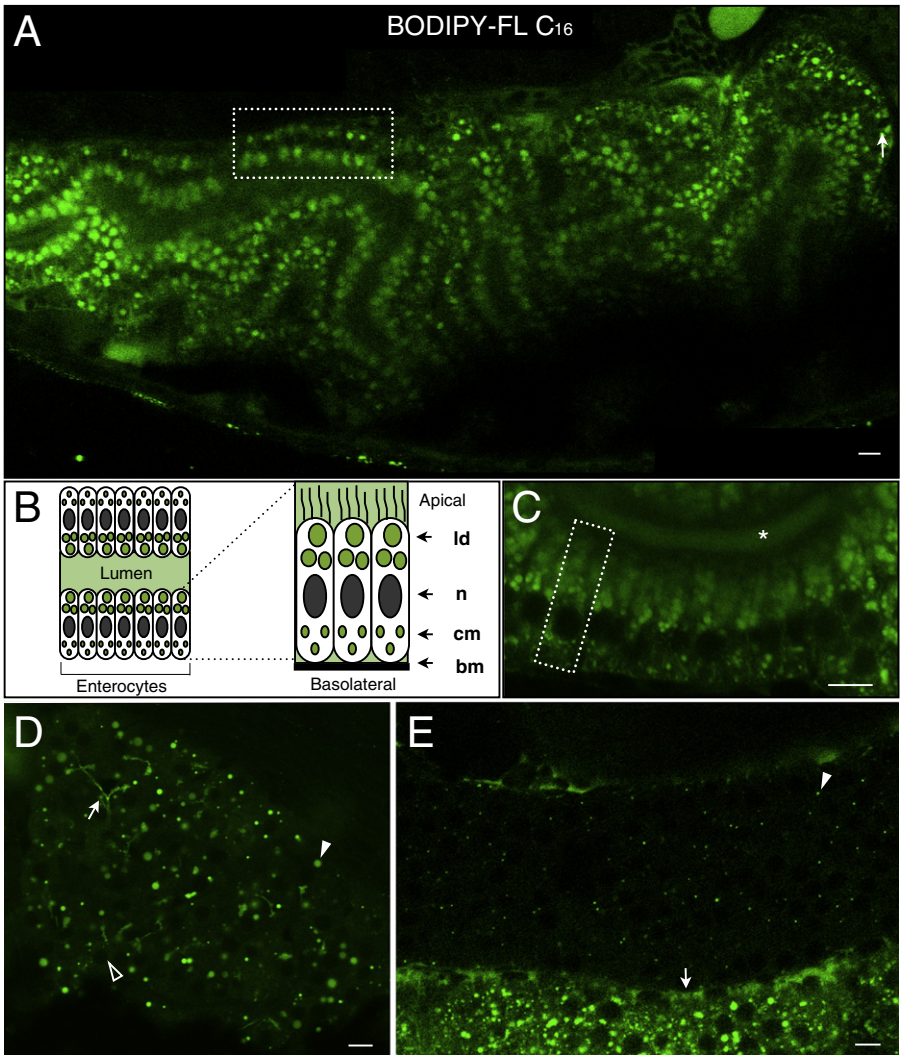

Fig. 1. BODIPY-FL C_{16} accumulates in lipid droplets in the digestive organs of live larval zebrafish. In all images, anterior is to the right to allow liver viewing. A. Enterocytes of the anterior intestinal bulb readily absorb BODIPY-FL C_{16} following an egg yolk and analog feed. The dotted box indicates a row of intestinal enterocytes exhibiting apical and basolateral accumulation of BODIPY-FL C_{16}. Larger gaps in intestinal fluorescence (arrow) are likely non-absorbing enteroendocrine cells (Wallace et al., 2005). B. A schematic of lipid metabolism in polarized intestinal enterocytes. Enterocytes take up lipids from the intestinal lumen, form lipid droplets (ld) and secrete basolateral chylomicrons (cm). The basement membrane (bm) and cell nucleus (n) are also indicated. C. Intestinal enterocytes (dotted box indicates a single enterocyte) of larvae fed BODIPY-FL C_{16} display apical lipid droplets and smaller basolateral fluorescent foci reminiscent of chylomicrons. The intestinal lumen is indicated (asterisk). D. BODIPY-FL C_{16} accumulates within large hepatic lipid droplets (filled arrowhead) and faintly in hepatic ducts (arrow). Hepatocyte nuclei (empty arrowhead) are also visible. E. BODIPY-FL C_{16} accumulates throughout the exocrine pancreas, forming small fluorescent foci (arrowhead). Beneath the exocrine pancreas, an intestinal blood vessel (arrow) running the length of the intestine fluoresces, indicating analog entry into the vascular system. A is a composite of 3 separate confocal images. Scale bars = 10μm. (n = 3; 6 larvae per feed.)

this technique to assess digestive organ function in a known digestive mutant, *fat-free*. Analog feeding confirms the morphological defects previously identified in this mutant and reveals a bile secretion defect, further implicating Fat-free in secretory vesicle trafficking (Ho et al., 2006).

Materials and methods

Zebrafish strains and fish maintenance

All experiments were carried out using zebrafish larvae (AB strain) at 6 dpf. Thin layer Chromatography (TLC) analysis was performed using Farber wildtype (FWT) larvae (6 dpf). The FWT line was created to increase the fecundity of the AB stock and is the product of an AB line outcrossed to a pet store line, which was then inbred over several generations. Larvae were maintained in accordance with the Carnegie Institution's Animal Care and Use Committee Protocol (#139). Homozygous mutant *fat-free* larvae were identified phenotypically using a previously described hypopigmentation assay (Ho et al., 2006) and deflated swim bladders (Farber et al., 2001).

Fluorescent analogs

All BODIPY analogs used in this study were obtained from Invitrogen and stored at stock concentrations in chloroform at −80 °C. The following green fluorescent BODIPY analogs were used to visualize FA metabolism in larval zebrafish: BODIPY-FL C_{16} (D-3821), BODIPY-FL C_{12} (D-3822), BODIPY-FL C_5 (D-3834), BODIPY-FL C_2 (D-2183), and BODIPY $_{493/503}$ (D-3922). For all feedings, the BODIPY analogs were evaporated under a stream of Nitrogen gas and resuspended in 200 proof ethanol (5–10 μL) in Eppendorf tubes. Zebrafish embryo medium (EM; 90–95 μL) was added to the resuspended solution. The resulting fluorescent stock solutions were protected from light with aluminum foil, as were the larvae during feeding in plastic 6-well culture plates. The BODIPY fluorophore is 2–3 carbon lengths long, effectively making the analogs longer than their chain length designation. Additionally, high concentrations of the green BODIPY fluorophore can self-quench or red shift due to excimer formation and this should be considered if cofeeding analogs that emit in the red spectr or when using transgenic larvae (Pagano et al., 1991).

Preparation and feeding of fluorescent liposomes

To make the fluorescentum vesicle feeding solution, a 5% egg yolk emulsion was prepared with zebrafish EM. 1 mL of frozen chicken egg yolk (Land O' Lakes brand eggs) was thawed to room temperature and mixed with zebrafish EM (19 mL). The resulting mixture was pulse sonicated with a 1/4th inch tapered microtip (5 s total processing time, 1 s on, 1 s off, output intensity: 3 W) continuously for 2 min (Sonicator Ultrasonic Processor 6000, Misonix Inc., Farmingdale, New York, USA). The resuspended BODIPY analog was quickly added to 5 mL of the emulsion and vortexed for 30 s for a final concentration of 6.4 μM BODIPY-FL. Vesicle formation was confirmed by viewing 10–20 μL of the solution between coverslips using confocal microscopy (Fig. S1 in supplementary material). For administering BODIPY-FL analogs in the absence of egg yolk, the resuspended analogs were added to 1 mL of 5% FA-free bovine serum albumin (BSA; cat. # A8806-5G, Sigma) and pipetted several times to mix well. To this solution, 4 mL of zebrafish EM was added and mixed well. Before liposome feeding, larvae were screened for signs of developmental delay (*e.g.*, unabsorbed yolk, deflated swim bladder, malformed jaw) or abnormal digestive organ morphology. Twenty larvae were placed in 5 mL of the fluorescent vesicle solution and fed in a 6-well culture dish on a slowly moving orbital shaker for 4–8 h. We did not detect any obvious signs of toxicity during feeding. After feeding, larvae were washed several times in EM to remove residual label, anesthetized with MESAB, and live mounted for imaging in a small volume of 3% methylcellulose solution under a coverslip.

Microscopy

Imaging was performed using an SP2 confocal microscope (Leica Microsystems, Deerfield, Illinois, USA) with an Argon laser under a 63× oil objective. To image FA accumulation in multiple digestive organs it was often necessary to merge several single images together.

Synthesis of BODIPY standards

In addition to the BODIPY-FL analogs, the following BODIPY-tagged lipids (Invitrogen, Inc.) were used as TLC standards: three BODIPY-phosphatidylcholines (a- BODIPY $_{530/550}$-C5-HPC (D3815); a- BODIPY $_{530/550}$-C12-HPC, (D3792); and a- BODIPY $_{530/550}$-C16-HPC (D7707 discontinued)) and BODIPY-cholesteryl (cholestryl- BODIPY-FL C_{12}, (C3927MP)). BODIPY-tagged triacylglyceride (BODIPY-TAG) and diacylglyceride (BODIPY-DAG) standards are not commercially available at the time and were synthesized *in vitro*.

To synthesize BODIPY-DAG standards of different chain lengths, we utilized phospholipase C (PLC, P-9439, Sigma) to enzymatically cleave the phosphatidylcholine moieties from BODIPY-C_{16}-HPC, BODIPY-C_{12}-HPC, and BODIPY-C_5-HPC analogs (Farber et al., 1999). PLC was dissolved in 20 mM Tris, 10 mM $CaCl_2$, pH 7.5 at a stock concentration of approximately 1 Unit/μL. To synthesize BODIPY-DAG, approximately 50 μg of the desired BODIPY-PC (either -C_5, -C_{12}, or -C_{16}) was dried down with nitrogen gas and resuspended in ethanol (10 μL, 200 proof). PLC enzyme (20 Units) and EM (80 μL) were added to the BODIPY-PC substrate solution, mixed well, and incubated at 37 °C for 5 h. All DAG synthesis reactions were stopped by chloroform: methanol:water (2:1:1 v/v) extraction. The resulting organic phase was dried down with nitrogen gas, resuspended in ethanol (20 μL), and stored at −20 °C. Reaction efficiency was assayed using TLC and an ethyl ether/benzene/ethanol solvent system (8:13.5:0.5 v/v). TLC analysis revealed that generation of BODIPY-DAG by PLC-mediated cleavage of BODIPY-PC proceeded nearly to completion, with very little remaining substrate detected (data not shown).

To generate BODIPY-TAG from newly synthesized BODIPY-DAG, we generated mouse liver microsomes containing the TAG-synthesizing enzyme acyl CoA diacylglycerol transferase (Dgat) (Yu et al., 2010). Briefly, liver tissue (0.2 g) from a fasted mouse (Black 6 strain) was homogenized in ice-cold buffer (100 mM sucrose, 50 mM potassium chloride, 30 mM EDTA, 40 mM monopotassium phosphate, pH 7.2) and centrifuged (10,000×*g* in a Beckman L8-M Ultracentrifuge, SW41 rotor) for 15 min at 4 °C. To pellet Dgat-containing microspheres, the supernatant was collected and recentrifuged (100,000×*g* in an Optima TLX Ultracentrifuge) for 70 min. The microspheres were aliquoted, flash frozen in liquid nitrogen, and stored at −80 °C. The TAG synthesis reaction was prepared by first drying down the volume equivalent of 40 μg of BODIPY-DAG with nitrogen gas. Acetone (10 μL) and reaction buffer (312 μL of 100 mM Tris–HCl, pH 7.5, 150 mM magnesium chloride, 1.25 mg/mL FA-free BSA, 200 mM sucrose, 1 mM EDTA) were added. The mixture was pulse sonicated (6×3 second pulses, output intensity 2 W). Palmitoyl Coenzyme A (4 μL of a 1 mM stock) and liver microsomes (10 μg) were added to the reaction mixture and incubated at 37 °C for 2 h. Total lipids were extracted and separated by TLC as described. Although TLC analysis revealed BODIPY-TAG synthesis to be relatively inefficient (data not shown), a sufficient amount of BODIPY-TAG was produced for use as a TLC standard.

Fluorescent thin layer chromatography

To determine if BODIPY-FL analogs are metabolized by zebrafish larvae, TLC analysis was performed on larval lipid extracts. Lipids were extracted from 60 larvae that had been fed BODIPY-FL C_{16},

-C_{12}, -C_5. -C_2, or BODIPY$_{493/503}$ in the presence or absence of egg yolk. Following a 4–8 h incubation in liposomes, larvae were washed several times with EM to remove trace amounts of the feeding solution, pelleted on ice, and pulse sonicated in 500 μL of cold (4 °C) EM. Total lipids were extracted from larval homogenates, as described above. The organic phase was collected and stored at −80 °C in brown glass vials (National Scientific, Rockwood, Tennessee, USA) until TLC analyses were performed.

A two-solvent system was used to resolve BODIPY metabolites present in extracted samples. The first polar solvent system (chloroform/ethanol/triethylamine/water (30:34:30:8 mL) separated phospholipids and BODIPY-FL. The second solvent system (petroleum ether/ethyl ether/acetic acid) (45:5:0.5 mL) resolved TAG from cholesterol ester (CE) and BODIPY$_{493/503}$. Solvent systems were added to TLC chambers and allowed to equilibrate for at least 20 min prior to sample separation. Samples and BODIPY standards were spotted onto silica gel TLC plates (Whatman, LK5D; EMD Biochemicals) and dried for several minutes. Following tank equilibration, plates containing the samples were run until the solvent front reached 1 cm from the top of the plate. After drying, plates were scanned (Storm Scanner 860; Molecular Dynamics, USA) using the blue fluorescence laser (excitation: 450 nm; emission: 520LP; PMT 800 V, 200 m pixel size) to detect fluorescent bands.

Results and discussion

In this study we selected four BODIPY-tagged FA analogs to administer to zebrafish larvae: the short chain acetic acid (BODIPY-FL C_2), the medium chains pentanoic (BODIPY-FL C_5) and lauric acid (BODIPY-FL C_{12}), and the long chain palmitic acid (BODIPY-FL C_{16}). We also administered the nonmetabolizable BODIPY fluorophore (BODIPY $_{493/503}$) to determine to what degree the fluorophore alone could visualize FA metabolism.

To deliver BODIPY-FL analogs to larval zebrafish, we simulated a high-fat diet by administering the analogs in chicken egg yolk liposomes. Previous studies in adult (Marza et al., 2005) and larval (Walters et al. submitted) zebrafish have reported the increased appearance of intestinal lipid droplets and the upregulation of FA metabolism genes following an egg yolk meal. Liposomes were made by sonicating chicken egg yolk to disperse yolk lipid aggregates, which reform into small, more homogeneous vesicles (Finer et al., 1972).

BODIPY-FL analogs partition into different liposomal compartments

Following addition to sonicated egg yolk, BODIPY-FL analogs partition into distinct liposomal compartments (Fig S1). BODIPY-FL C_{16} liposomes appear as rings in confocal images, indicating analog partitioning into the liposomal membrane. BODIPY-FL C_{12}, C_5, and C_2 partition into the aqueous core of liposomes, which appear as fluorescent ovals in confocal images (Fig S1). BODIPY $_{493/503}$ also partitions into the liposome interior.

The BODIPY fluorophore does not recapitulate fatty acid metabolism in larval zebrafish

When administered to zebrafish larvae, the BODIPY fluorophore first accumulates in intestinal lipid droplets in the anterior intestine, then gradually accumulates in the hepatic ducts over time (Fig. S2). Previous studies in medaka (*Oryzias latipes*) have shown that this fluorophore accumulates in the gall bladders, intrahepatic biliary systems, and intestines of larvae soaked in the fluorophore at the early morula stage (Hornung et al., 2004). The apparent exclusion of BODIPY from hepatic lipid droplets suggests that the fluorophore's lack of an acyl chain hinders its hepatic uptake. Interestingly, the fluorophore itself readily enters intestinal lipid drops, suggesting differential FA import mechanisms in the intestine and liver.

BODIPY-FL analog feeding visualizes FA metabolism in zebrafish larvae

To better visualize FA metabolism, we selected four different chain length BODIPY FA analogs to administer to zebrafish larvae. We reasoned that fluorescent analogs that mimicked short, medium, and long chain saturated FAs would be metabolized similarly to their native counterparts and more faithfully recapitulate FA metabolism. Saturated BODIPY-FL analogs are poorly metabolized by cultured cells (Huang et al., 2004; Thumser and Storch, 2007), prompting some to utilize BODIPY-FL as nonmetabolizable analogs (Atshaves et al., 2004; Huang et al., 2004); however, BODIPY-FL C_{12} has been shown to be metabolized by the parasitic worm *Schistosoma mansoni* (Furlong et al., 1995), suggesting endogenous factors absent in cultured cell models (*e.g.*, bile, gut microbes) are necessary for appreciable BODIPY-FL metabolism.

When administered to zebrafish larvae, long, medium, and short chain BODIPY-FL analogs accumulate in distinct subcellular patterns in larval digestive organs (Figs. 1–4). Following a liposome feed, analogs appear sequentially in the digestive organs of larvae, accumulating in the intestine first (1–2 h feed), then the liver (2–4 h feed), and finally in the pancreas (4–6 h feed).

BODIPY-FL C_{16}

BODIPY-FL C_{16} appears throughout the intestine of larval zebrafish (Fig. 1), accumulating in apical and basolateral domains of intestinal enterocytes (Fig. 1A). Fluorescent lipid droplets form in the lumenal side of enterocytes, while small, fluorescent foci appear in the basolateral region (Fig. 1C), revealing these cells to be functionally polarized. The polarity of BODIPY-C_{16} accumulation in intestinal enterocytes is highly reminiscent of the apical lipid droplets and basolateral chylomicrons seen in electron micrographs of larval zebrafish enterocytes fed a high-fat diet (Walters et al., submitted). This functional polarity also coincides with the previously characterized appearance of apical and basolateral specific proteins in enterocytes, including the apical tight junction marker ZO-1 and the basolateral transporter sodium potassium ATPase (Wallace and Pack, 2003; Wallace et al., 2005). In addition, fluorescent lipid droplets appear in the livers and exocrine pancreases of BODIPY-C_{16} fed larvae (Fig. 1D, E). The appearance of BODIPY-C_{16} in intestinal, hepatic, and pancreatic lipid droplets suggests that unlike the BODIPY fluorophore, this FA analog is transported and metabolized similarly to native long chain FAs by zebrafish larvae.

BODIPY-FL C_{12}

Lipid droplets also appear in the digestive organs of larvae fed BODIPY-FL C_{12} (Fig. 2). Similar to BODIPY-FL C_{16}, apical and basolateral differences in lipid analog accumulation are apparent in larval enterocytes (Fig. 2A). Furthermore, analog feeding reveals a high degree of subcellular detail in the intestine, enabling single enterocytes to be clearly distinguished (Fig. 2A). More lipid droplets form in the livers and pancreases of BODIPY-FL C_{12} fed larvae (Fig. 2B, C), consistent with the faster absorption and metabolism of MCFAs. Accumulation of the analog in the intestinal lumen suggests expedited transport of the analog to the liver, drainage into hepatic ducts, and reentry into the intestinal lumen as bile (Fig. 2A). Studies done using the human parasite *Shistosoma masoni* have also found that BODIPY-FL C_{12} localizes to intracellular lipid droplets and membranes and is metabolized into neutral lipids and phospholipids (Furlong et al., 1995).

BODIPY-FL C_5

Larvae fed BODIPY-FL C_5 reveal a high degree of cellular and subcellular detail throughout their digestive systems (Fig. 3). Intestinal enterocytes exhibit apical lipid droplets and basolateral analog accumulation consistent with sites of lipoprotein secretion (Andre et al., 2000) (Fig. 3A, B). Intestinal absorption of the analog decreases in

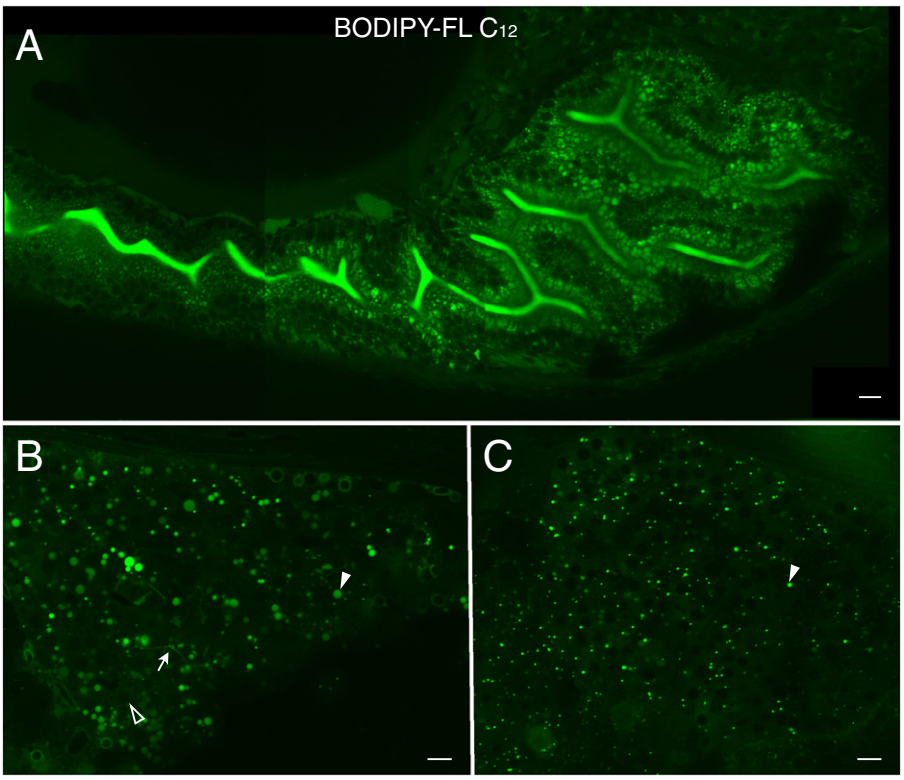

Fig. 2. BODIPY-FL C_{12} is absorbed and transported in the digestive organs of zebrafish larvae. A. The analog appears in the intestinal lumen as well as in lipid droplets in intestinal enterocytes. Diffuse cellular accumulation of BODIPY-FL C_{12} is consistent with the analog's shorter chain length, decreased hydrophobicity, faster metabolism, and entry into more subcellular compartments. B. BODIPY-FL C_{12} readily accumulates in the liver, visualizing large lipid droplets (filled arrowhead), hepatic ducts (arrow), and hepatocyte nuclei (empty arrowhead). C. BODIPY-FL C_{12} accumulates in fluorescent foci (arrowhead) in the exocrine pancreas. A Scale bars = 10μm. (n = 3; 6 larvae per feed.)

the distal segment of the intestine, reflecting differences in cellular composition (Wallace et al., 2005) and gene expression (Andre et al., 2000) along the length of the intestine (data not shown). Different intestinal cell types can be identified by their inability to absorb the fluorescent analogs, and are likely hormone-secreting enteroendocrine cells in the anterior intestine and mucosal cells in the posterior intestine (Wallace et al., 2005).

In the liver, BODIPY-FL C_5 reveals many subcellular details including lipid droplets and hepatocyte nuclei (Fig. 3E), as well as the hepatic ductal network (Fig. 3D and Supplementary Movie 1). Previous work done in medaka fish has shown that larval exposure to BODIPY-FL C_5 in an aqueous bath is sufficient to visualize the hepatobiliary network, enabling analysis of ductal morphology, hepatobiliary transport, and hepatotoxicity *in vivo* (Hardman et al., 2008). In our assay, analog delivery via a high-fat diet enhances BODIPY FL uptake and metabolism, allowing more BODIPY-Fl C_5 to be metabolized and incorporated into subcellular structures.

In the exocrine pancreases of BODIPY-FL C_5 fed larvae, zymogen granules are observed in acinar cells, as well as pancreatic ducts (Fig. 3C). The wealth of subcellular details observed in the digestive organs of larvae fed BODIPY-FL C_{12} and C_5 reflects the expedited metabolism of medium chain FAs (MCFA) (reviewed in Papamandjaris et al., 1998) and makes these two analogs particularly well suited for use as vital dyes. In addition, the preference of acyl-CoA synthetases for LCFA likely permits some MCFA to bypass TAG synthesis, enter the blood, and travel directly to the liver via the portal vein (Bach et al., 1996; Bloom et al., 1951).

BODIPY-FL C_2

In contrast to the M- and LCFA analogs, BODIPY-FL C_2 does not enter lipid droplets in larval digestive organs and instead accumulates in the intestinal lumen, intrahepatic biliary system, and pancreatic ducts (Fig. 4). The diffuse cytoplasmic fluorescence observed in cells of BODIPY-FL C_2 fed larvae suggests the analog is excluded or actively exported from cells. SCFAs are produced mainly by carbohydrate fermentation in the large intestine, with acetate (C2:0), propionate (C3:0), and butyrate (C4:0) being the main SCFAs generated (Cummings and Macfarlane, 1991). Although SCFAs are not typically utilized for TAG synthesis, they can be used to make glycerol. We find no imaging evidence of BODIPY-FL C_2 incorporation into TAG containing lipid droplets in fed zebrafish larvae, suggesting that this analog is not appreciably metabolized. Interestingly, the addition of a 2-carbon length acyl chain to the BODIPY fluorophore drastically sways its accumulation pattern from hydrophobic lipid droplets to more hydrophilic environments. We hypothesize that the addition of a short acyl chain to BODIPY creates a more amphipathic BODIPY-FL C_2 analog that can self-associate, possibly retarding its movement across cellular membranes.

Egg yolk feeding enhances the metabolism of BODIPY-FL analogs

To determine whether zebrafish larvae metabolize BODIPY-FL, we analyzed lipid extracts from fed larvae using TLC. We first determined the effect of egg yolk feeding on larval uptake and metabolism of BODIPY-FL by administering the analogs in the presence and absence of egg yolk. TLC analysis reveals that BODIPY-FL analogs remain largely unmetabolized when administered without of egg yolk (Fig. 5, lanes 1–6). Prominent bands in the BODIPY-FL C_{16} and BODIPY-FL C_{12} unfed lanes correspond to ingested but unmetabolized analogs. The increased fluorescence intensity of the unmetabolized bands present in the BODIPY-FL C_{16}, BODIPY-FL C_{12}, and BODIPY unfed lanes indicates that the analog pool does not become diluted by yolk lipids in unfed larvae (compare lanes 1, 2 and 5 with 7, 8 and 11).

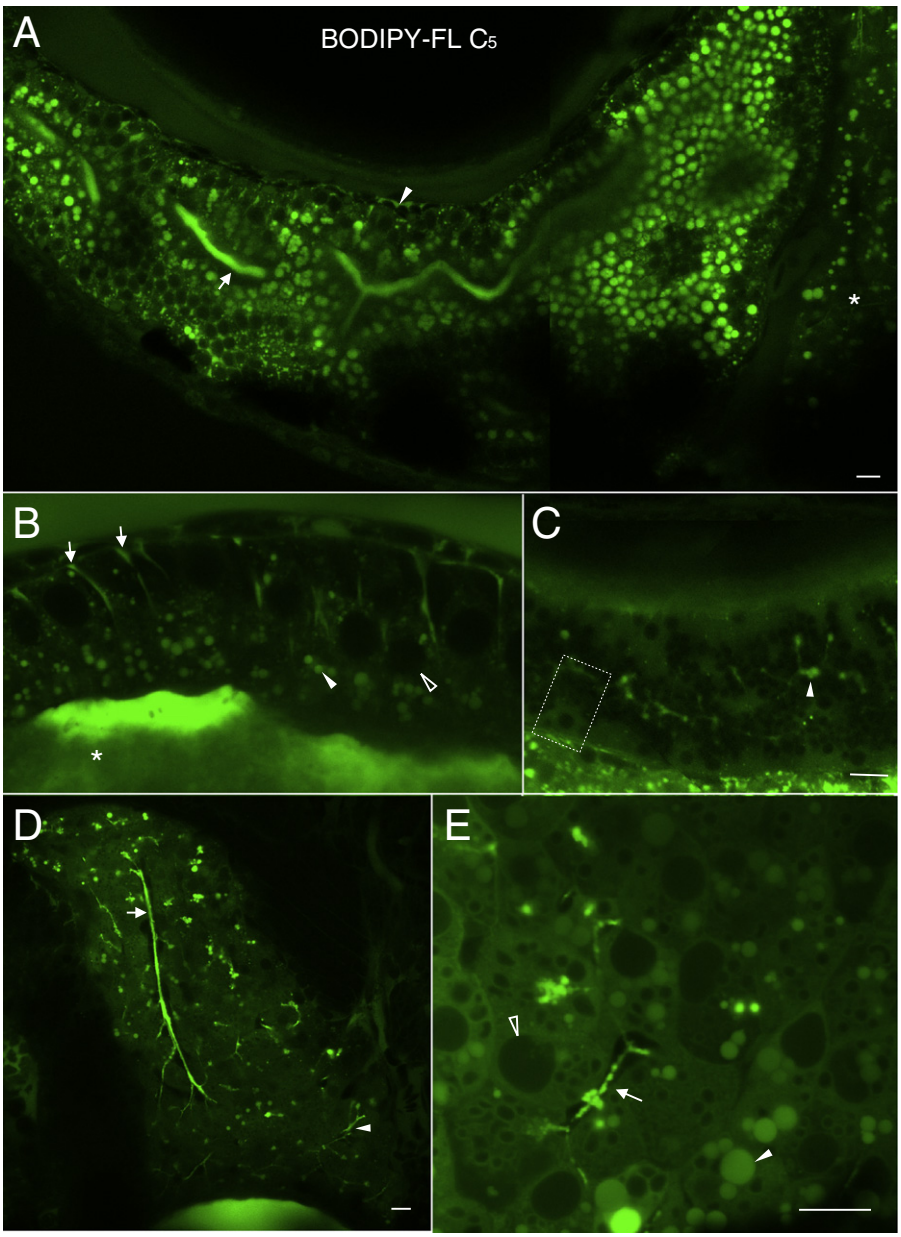

Fig. 3. BODIPY-FL C_5 reveals significant subcellular details within larval digestive organs (6dpf). A. In enterocytes of the anterior intestine BODIPY-FL C_5 appears in structures reminiscent of lipid droplets. Lumenal accumulation of BODIPY-FL C_5 in the intestine (arrow) is consistent with the expedited metabolism, transport and biliary concentration of medium chain fatty acids. The analog also appears in a dorsal intestinal blood vessel (arrowhead) and in the liver (asterisk). B. Subcellular enterocyte morphology is visualized following a BODIPY-FL C_5 feed. Lipid droplets (filled arrowhead), a nucleus (empty arrowhead), apparent pericellular accumulation of the analog (arrows) and the intestinal lumen (asterisk) are indicated. C. BODIPY-FL C_5 visualizes subcellular details of acinar cells and pancreatic ducts in the larval exocrine pancreas. A single acinar cell (dashed box) containing a basal nucleus and apical zymogen granules, as well as pancreatic ducts (arrowhead) is indicated. D. BODIPY-FL C_5 feeding illuminates the intrahepatobiliary ductal network. In the right liver lobe, a single long duct (arrow), numerous interconnecting ducts and terminal ductules (arrowhead) are illuminated (see also Supplementary Movie-1). E. Subcellular details of larval hepatocytes are revealed by BODIPY-FL C_5 feeding. Lipid droplets (filled arrowhead), hepatocyte nuclei (empty arrowhead), and intrahepatic ducts (arrow) are indicated. A. is a composite of 2 separate confocal images. Scale bars = 10μm. (n = 3; 6 larvae per feed.)

In contrast, zebrafish larvae fed egg yolk show enhanced metabolism of BODIPY-FL (Fig. 5, lanes 7–12). Fed larvae readily metabolize long and medium chain BODIPY-FL when fed with egg yolk (Fig. 5, lanes 7–9). Confocal imaging of yolk-fed and unfed larvae administered BODIPY-FL C_{16} confirms that the addition of egg yolk increases analog uptake and lipid droplet formation in the intestine and liver (Fig. S3).

Several factors likely enable the BODIPY-FL analogs to be metabolized by zebrafish larvae. In our assay, larvae are fed for 4–8 h, enabling high amounts of analog to be continuously delivered. In addition, feeding is known to trigger metabolic responses (*e.g.,* insulin secretion, transcriptional upregulation of catabolic genes, and nutrient transporter trafficking to the plasma membrane) in an organism. By feeding the BODIPY-FL analogs with egg yolk, we trigger a physiological feeding response, which maximizes FA uptake and metabolism. Furthermore, bile is critical for FA digestion and is pumped directly into the intestinal lumen in response to food consumption. By enhancing bile production through the feeding of a high-fat meal, we increase FA analog solubility and subsequent absorption by intestinal enterocytes.

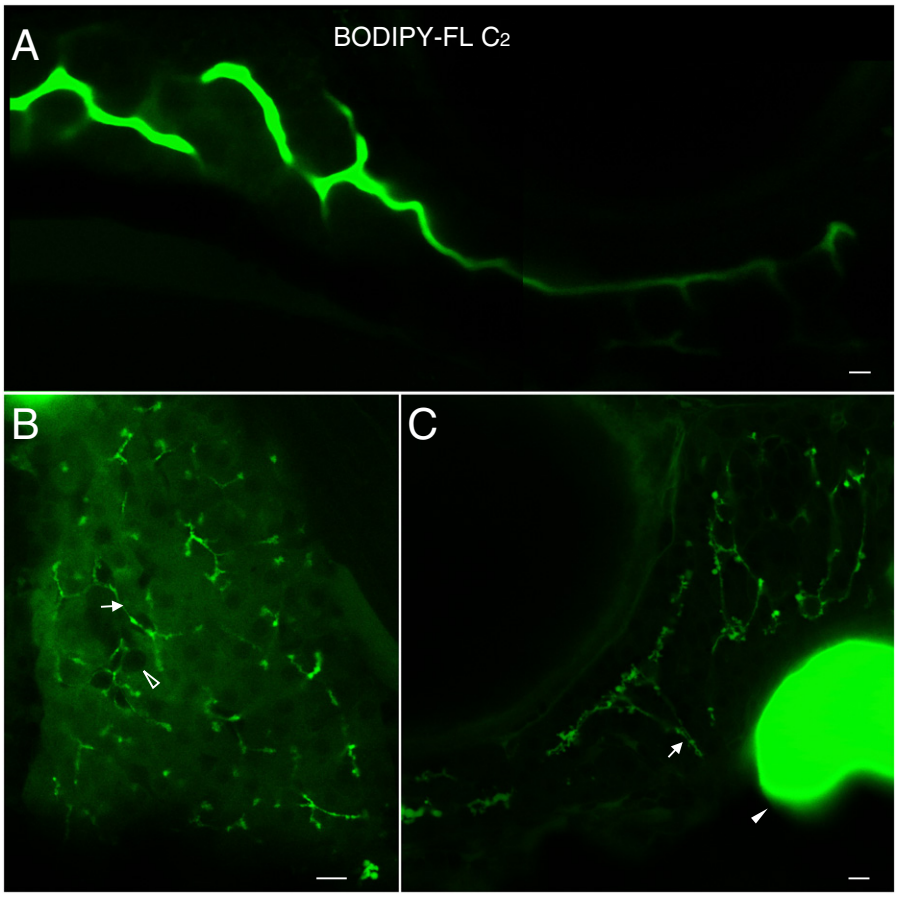

Fig. 4. BODIPY-FL C_2 does not participate appreciably in lipid metabolism. A. Unlike the longer chain length analogs, BODIPY-FL C_2 fluorescence appears primarily in the intestinal lumen of larvae. B. In the liver BODIPY-FL C_2 accumulates in the hepatic ducts (arrow) and diffusely in hepatocytes, whose nuclei are discernable (empty arrowhead). C. The ductal network of the exocrine pancreas is also labeled (arrow). The gall bladder (filled arrowhead) is indicated in C. A. is a composite of 2 separate confocal images. Scale bars = 10μm. (n = 3; 6 larvae per feed).

Zebrafish larvae metabolize BODIPY-FL C_{16} into neutral lipids

TLC analysis confirms that BODIPY-FL C_{16} is predominantly metabolized into triacylglycerol (TAG) (Fig. 5, lane 7; Fig. 6, lane 1), consistent with its appearance in neutral lipid-containing lipid droplets and presumed lipoproteins. Surprisingly, the analog is not appreciably metabolized into phospholipids, as would be predicted given that palmitate (C16:0) and stearate (C18:0) are the predominant saturated FAs in phospholipids (reviewed by Moore, 1982). Caco-2 cells readily incorporate radiolabeled palmitic acid into phospholipids (van Greevenbroek et al., 1995), though studies have shown that the rate of phospholipid synthesis is less susceptible to diet, and remains relatively constant, in contrast to triacylglyceride synthesis (Iritani et al., 1976). Furthermore, fasting, as well as increased availability of palmitate, stimulates triglyceride synthesis more so than phospholipid synthesis, suggesting these lipogenic processes are regulated independently (Iritani et al., 1976). While we do not know why zebrafish larvae preferentially metabolize BODIPY-FL C_{16} into neutral lipids, we suspect native yolk-derived palmitate outcompetes BODIPY-FL C_{16}. The BODIPY fluorophore is known to affect membrane partitioning and metabolism of lipid analogs (Baumgart et al., 2007; Karsenty et al., 2009), and likely causes the BODIPY-FL C_{16} analog to be metabolized differently than native palmitic acid by zebrafish larvae.

Zebrafish larvae metabolize BODIPY-FL C_{12} and BODIPY-FL C_5 into complex lipids

Of the analogs tested, BODIPY-FL C_{12} and BODIPY-FL C_5 are metabolized to the greatest extent. Both analogs are synthesized into triacylglycerides (Fig. 5, lanes 8, 9; Fig. 6, lanes 2, 3) and phosphatidylcholine (Fig. 5, lanes 8, 9). Interestingly, unlike BODIPY-FL C_{16}, the 12 carbon BODIPY-FL C_{12} analog is metabolized into phospholipids, suggesting this MCFA analog is metabolized more like a LCFA due to its flurophore-lengthened acyl chain. The multiple fluorescent bands that appear at decreasing 2-carbon length increments below the unmetabolized bands (Fig. 5, lanes 7–9) are likely the products of lipid catabolism, indicating that the analogs can be burned as sources of cellular fuel. MCFAs enter mitochondria independently of the carnitine transport system (Friedman et al., 1990), thus BODIPY-FL C_{12} and BODIPY-FL C_5 may be short enough to directly enter the mitochondria to be oxidized. The greater metabolic usage of BODIPY-FL C_{12} and BODIPY-FL C_5 parallels the high degree of subcellular detail apparent following larval feeding and confocal imaging.

Zebrafish larvae do not metabolize BODIPY-FL C_2

Unlike the longer chain length analogs, zebrafish larvae do not metabolize BODIPY-FL C_2, with little to no analog appearing in complex lipids (Fig. 5, lane 11; Fig. 6, lane 4). This is consistent with BODIPY-FL C_2 fed larvae never exhibiting fluorescent lipid droplets in their digestive organs or lipid-accumulating tissues, concentrating the analog primarily in the intestinal lumen and hepatic and pancreatic ducts (Fig. 4). The differential metabolism of short chain FAs (SCFA) is likely due to the preference of metabolic enzymes that process and transport FAs for longer chain length FAs (Hall et al., 2003; Hall et al., 2005; Stahl et al., 1999; Steinberg et al., 1999). As expected, the BODIPY fluorophore is not metabolized by zebrafish into complex lipids (Fig. 5 lanes 5, 11), despite its accumulates in intestinal lipid drops.

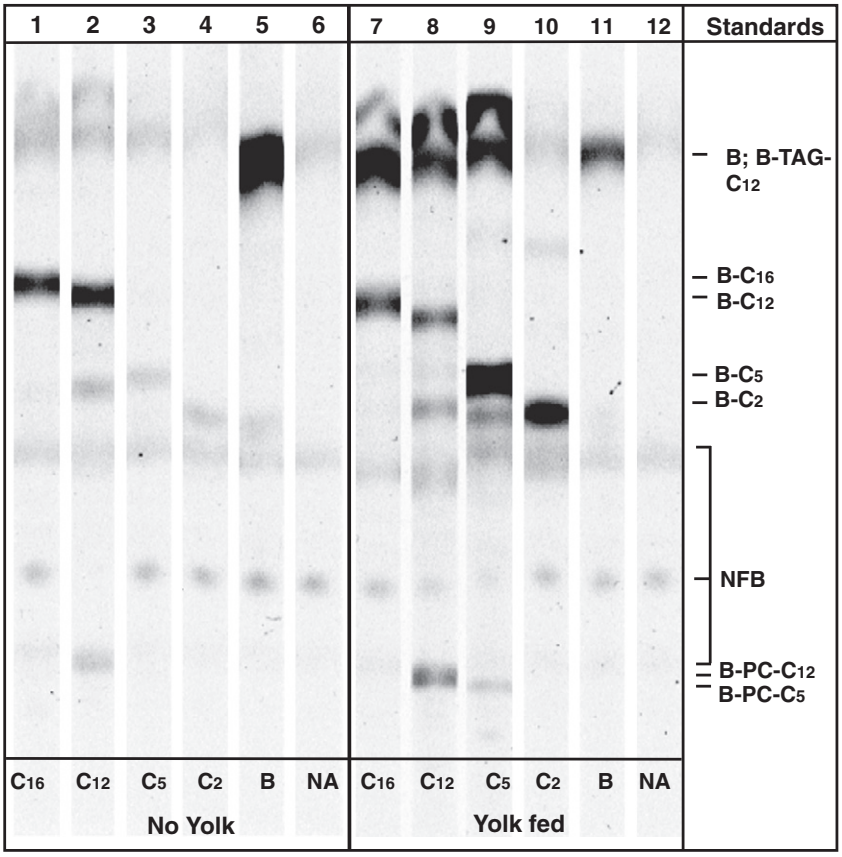

Fig. 5. Egg yolk feeding enhances the uptake and metabolism of BODIPY fatty acid analogs by zebrafish larvae. Thin layer chromatography analysis of total larval lipids extracted following analog feeds in the absence (lanes 1–5) and presence (lanes 7–11) of egg yolk. Lanes 6 and 12 are no analog (NA) unfed and yolk fed controls, respectively, and exhibit faint naturally fluorescent lipid bands (NFB). A polar solvent system was used to resolve fluorescent phospholipids (bottom of plate), free analogs (middle), and neutral lipids (top of plate). Abbreviations for fluorescent lipid standards are as follows: BODIPY-Cholesteryl (B-CE-C_{12}), BODIPY-Triacylglyceride (B-TAG-C_{12}), $BODIPY_{493/503}$ (B), BODIPY-C_{16} (B-C_{16}), and BODIPY-Phosphatidylcholine (B-PC-C_{12}, B-PC-C_5).

In summary, the TLC results confirm that the uptake and transport of the BODIPY-FL analogs observed in live zebrafish larvae reflect metabolic events specific to FAs (*e.g.*, neutral and phospholipid synthesis, β-oxidation). Furthermore, differences in the metabolites of each chain length BODIPY-FL show that these analogs partition into different metabolic pathways based on their chain length.

BODIPY-FL C_5 feeding reveals a bile secretion defect in fat-free larvae

To demonstrate the utility of BODIPY-FL analogs to functionally evaluate digestive mutants, we fed the previously identified mutant, *fat-free* (*ffr*) (Farber et al., 2001). Larvae with a mutation at the *ffr* locus exhibit reduced lipase activity and cholesterol absorption as well as abnormal hepatic ducts and bile canaliculi (Ho et al., 2006), suggesting a defect in bile secretion. To determine if bile secretion is the basis for the *ffr* phenotype, we administered BODIPY-FL C_5 liposomes to these larvae. Fed *ffr* larvae exhibit apparent abnormal bile accumulation in their hepatocytes (Fig. 7). Therefore, reduced lipase activity and cholesterol absorption in *ffr* larvae likely results from a bile secretion defect, due to the failure of canalicular and ductal networks to properly drain bile into the gall bladder. The cholestatic phenotype observed in *ffr* mutants is also consistent with the ultrastructural defects observed in the Golgi of hepatocytes and biliary cells of *ffr* larvae (5 dpf) (Ho et al., 2006). The Ffr protein is predicted to have a Dor-1 like domain characteristic of conserved oligomeric golgi (COG) complex proteins that are essential for glycosylation events and vesicular trafficking. Thus, *ffr* may be required for proper Golgi-related vesicular trafficking of bile transporters, such that in *ffr* mutants, bile transporters cannot be properly trafficked to the plasma membrane (Liu et al., 2010).

Conclusion

We have developed a feeding assay that allows FA metabolism to be visualized in live larval zebrafish. Yolk feeding enhances the uptake and metabolism of these analogs, allowing a comparative analysis of FA metabolism. Using this method we demonstrate that long, medium, and short chain BODIPY-tagged FAs are differentially metabolized by zebrafish larvae, revealing FA metabolism to be conserved in these teleosts. In addition, the distinct metabolism of each analog allows them to be

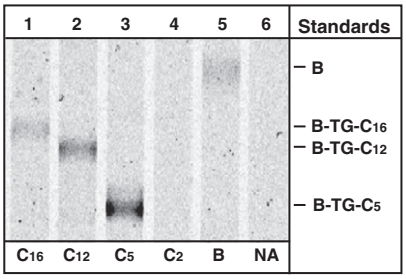

Fig. 6. Medium and long chain fatty acid BODIPY analogs are synthesized into triacylglyceride. A second protonating solvent system was used to separate $BODIPY_{493/503}$ (B) from BODIPY-Triacylglyceride (B-TAGs). Lipid extracts from larvae fed egg yolk without analog (NA) appear in lane 6. (n = 3 concurrent feeds).

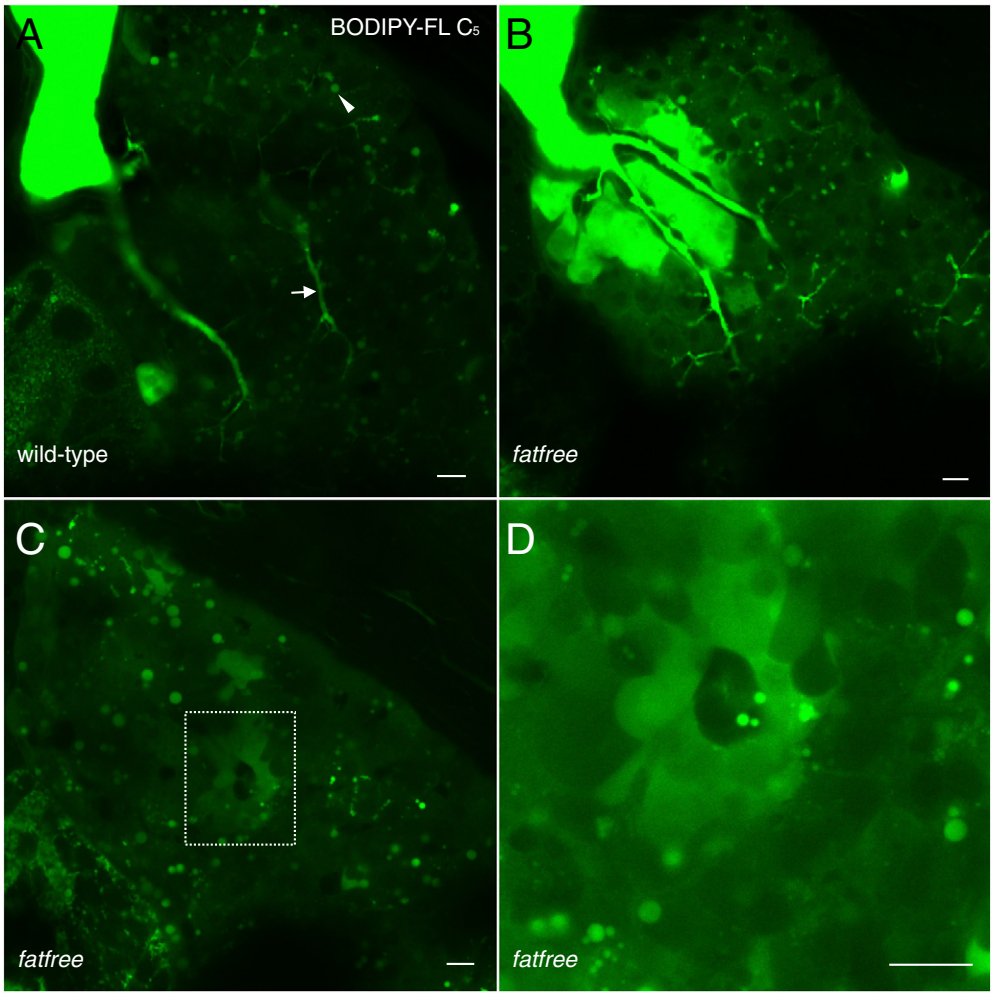

Fig. 7. Fat-free (ffr) larvae display abnormal bile accumulation upon BODIPY-FL C_5 feeding. A. Wildtype siblings (controls) from a cross of ffr +/− larvae (6dpf) exhibit normal hepatic accumulation of BODIPY-FL C_5 in lipid droplets (filled arrowhead) and hepatic ducts (arrow). B. Hepatic ducts in ffr −/− larvae leak or abnormally accumulate BODIPY-FL C_5, consistent with the hepatobiliary structural malformations previously identified in these mutants. C. Analog labeling also reveals ffr −/− hepatocytes are unable to secrete bile as indicated by the appearance of cholestatic livers. D. A higher magnification of C. reveals abnormal accumulation of bile in a single ffr −/− hepatocyte. Scale bars = 10μm. (n = 3 feeds; 10 larvae per feed).

exploited as vital dyes to characterize organ structure and metabolic function *in vivo*. BODIPY-FL C_2 and -C_5 are ideal for examining hepatic and pancreatic ductal morphology, offering an expedited way to screen for ductal mutants. BODIPY-FL C_5 and BODIPY-FL C_{12} reveal a tremendous amount of cellular detail in the intestine, liver, and pancreas and provide a way to live-image subcellular processes in these organs over time and at various developmental stages. BODIPY-FL C_{16} accumulation into lipid droplets and lipoproteins allows multiple fat storing organs and tissues to be monitored simultaneously *in vivo*. In addition, these analogs can serve as tools to assess the physiological effects of a specific mutation or drug treatment, as we have demonstrated using the *ffr* mutant, and will likely aid in the development of therapeutics for metabolic disorders.

Supplementary materials related to this article can be found online at doi:10.1016/j.ydbio.2011.09.010.

Acknowledgments

The authors acknowledge Jen Anderson, Rosa Miyares, and Vitor Bortolo de Rezende for technical assistance, editorial help and critical discussions. Steven Leach and Marnie Halpern also contributed significantly to the revision of this manuscript.

References

Andre, M., Ando, S., Ballagny, C., Durliat, M., Poupard, G., Briancon, C., Babin, P.J., 2000. Intestinal fatty acid binding protein gene expression reveals the cephalocaudal patterning during zebrafish gut morphogenesis. Int. J. Dev. Biol. 44 (2), 249–252.
Atshaves, B.P., Storey, S.M., Huang, H., Schroeder, F., 2004. Liver fatty acid binding protein expression enhances branched-chain fatty acid metabolism. Mol. Cell. Biochem. 259 (1–2), 115–129.
Bach, A.M., Hann, L.E., Brown, K.T., Getrajdman, G.I., Herman, S.K., Fong, Y., Blumgart, L.H., 1996. Portal vein evaluation with US: comparison to angiography combined with CT arterial portography. Radiology 201 (1), 149–154.
Baumgart, T., Hunt, G., Farkas, E.R., Webb, W.W., Feigenson, G.W., 2007. Fluorescence probe partitioning between Lo/Ld phases in lipid membranes. Biochim. Biophys. Acta 1768 (9), 2182–2194.
Benzonana, G., Desnuelle, P., 1965. Kinetic study of the action of pancreatic lipase on emulsified triglycerides. Enzymology assay in heterogeneous medium. Biochim. Biophys. Acta 105 (1), 121–136.
Black, D.D., 2007. Development and physiological regulation of intestinal lipid absorption. I. Development of intestinal lipid absorption: cellular events in chylomicron assembly and secretion. Am. J. Physiol. Gastrointest. Liver Physiol. 293 (3), G519–G524.
Bloom, B., Chaikoff, I.L., Reinhardt, W.O., Entenman, C., Dauben, W.G., 1950. The quantitative significance of the lymphatic pathway in transport of absorbed fatty acids. J. Biol. Chem. 184 (1), 1–8.
Bloom, B., Chaikoff, I.L., Reinhardt, W.O., 1951. Intestinal lymph as pathway for transport of absorbed fatty acids of different chain lengths. Am. J. Physiol. 166 (2), 451–455.
Cummings, J.H., Macfarlane, G.T., 1991. The control and consequences of bacterial fermentation in the human colon. J. Appl. Bacteriol. 70 (6), 443–459.
Ellis, J.M., Frahm, J.L., Li, L.O., Coleman, R.A., 2010. Acyl-coenzyme A synthetases in metabolic control. Curr. Opin. Lipidol. 21 (3), 212–217.

Elo, B., Villano, C.M., Govorko, D., White, L.A., 2007. Larval zebrafish as a model for glucose metabolism: expression of phosphoenolpyruvate carboxykinase as a marker for exposure to anti-diabetic compounds. J. Mol. Endocrinol. 38 (4), 433–440.

Farber, S.A., Olson, E.S., Clark, J.D., Halpern, M.E., 1999. Characterization of Ca2+ −dependent phospholipase A2 activity during zebrafish embryogenesis. J. Biol. Chem. 274 (27), 19338–19346.

Farber, S.A., Pack, M., Ho, S.Y., Johnson, I.D., Wagner, D.S., Dosch, R., Mullins, M.C., Hendrickson, H.S., Hendrickson, E.K., Halpern, M.E., 2001. Genetic analysis of digestive physiology using fluorescent phospholipid reporters. Science 292 (5520), 1385–1388.

Finer, E.G., Flook, A.G., Hauser, H., 1972. Mechanism of sonication of aqueous egg yolk lecithin dispersions and nature of the resultant particles. Biochim. Biophys. Acta 260 (1), 49–58.

Friedman, M.I., Ramirez, I., Bowden, C.R., Tordoff, M.G., 1990. Fuel partitioning and food intake: role for mitochondrial fatty acid transport. Am. J. Physiol. 258 (1 Pt 2), R216–R221.

Furlong, S.T., Thibault, K.S., Morbelli, L.M., Quinn, J.J., Rogers, R.A., 1995. Uptake and compartmentalization of fluorescent lipid analogs in larval Schistosoma mansoni. J. Lipid Res. 36 (1), 1–12.

Guo, Y., Walther, T.C., Rao, M., Stuurman, N., Goshima, G., Terayama, K., Wong, J.S., Vale, R.D., Walter, P., Farese, R.V., 2008. Functional genomic screen reveals genes involved in lipid-droplet formation and utilization. Nature 453 (7195), 657–661.

Hall, A.M., Smith, A.J., Bernlohr, D.A., 2003. Characterization of the Acyl-CoA synthetase activity of purified murine fatty acid transport protein 1. J. Biol. Chem. 278 (44), 43008–43013.

Hall, A.M., Wiczer, B.M., Herrmann, T., Stremmel, W., Bernlohr, D.A., 2005. Enzymatic properties of purified murine fatty acid transport protein 4 and analysis of acyl-CoA synthetase activities in tissues from FATP4 null mice. J. Biol. Chem. 280 (12), 11948–11954.

Hardman, R., Kullman, S., Yuen, B., Hinton, D.E., 2008. Non invasive high resolution in vivo imaging of alpha-naphthylisothiocyanate (ANIT) induced hepatobiliary toxicity in STII medaka. Aquat. Toxicol. 86 (1), 20–37.

Ho, S.Y., Lorent, K., Pack, M., Farber, S.A., 2006. Zebrafish fat-free is required for intestinal lipid absorption and Golgi apparatus structure. Cell Metab. 3 (4), 289–300.

Hornung, M.W., Cook, P.M., Flynn, K.M., Lothenbach, D.B., Johnson, R.D., Nichols, J.W., 2004. Use of multi-photon laser-scanning microscopy to describe the distribution of xenobiotic chemicals in fish early life stages. Aquat. Toxicol. 67 (1), 1–11.

Huang, H., Starodub, O., McIntosh, A., Atshaves, B.P., Woldegiorgis, G., Kier, A.B., Schroeder, F., 2004. Liver fatty acid-binding protein colocalizes with peroxisome proliferator activated receptor alpha and enhances ligand distribution to nuclei of living cells. Biochemistry 43 (9), 2484–2500.

Iqbal, J., Hussain, M.M., 2009. Intestinal lipid absorption. Am. J. Physiol. Endocrinol. Metab. 296 (6), E1183–E1194.

Iritani, N., Yamashita, S., Numa, S., 1976. Dietary control of triglyceride and phospholipid synthesis in rat liver slices. J. Biochem. 80 (2), 217–222.

Karsenty, J., Helal, O., de la Porte, P.L., Beauclair-Deprez, P., Martin-Elyazidi, C., Planells, R., Storch, J., Gastaldi, M., 2009. I-FABP expression alters the intracellular distribution of the BODIPY C16 fatty acid analog. Mol. Cell. Biochem. 326 (1–2), 97–104.

Lehner, R., Kuksis, A., 1995. Triacylglycerol synthesis by purified triacylglycerol synthetase of rat intestinal mucosa. Role of acyl-CoA acyltransferase. J. Biol. Chem. 270 (23), 13630–13636.

Liu, H.Y., Lee, N., Tsai, T.Y., Ho, S.Y., 2010. Zebrafish fat-free, a novel Arf effector, regulates phospholipase D to mediate lipid and glucose metabolism. Biochim. Biophys. Acta 1801 (12), 1330–1340.

Lorent, K., Yeo, S.Y., Oda, T., Chandrasekharappa, S., Chitnis, A., Matthews, R.P., Pack, M., 2004. Inhibition of Jagged-mediated Notch signaling disrupts zebrafish biliary development and generates multi-organ defects compatible with an Alagille syndrome phenocopy. Development 131 (22), 5753–5766.

Lowe, M.E., 2002. The triglyceride lipases of the pancreas. J. Lipid Res. 43 (12), 2007–2016.

Mak, H.Y., Nelson, L.S., Basson, M., Johnson, C.D., Ruvkun, G., 2006. Polygenic control of Caenorhabditis elegans fat storage. Nat. Genet. 38 (3), 363–368.

Manganaro, F., Kuksis, A., 1985a. Purification and preliminary characterization of 2-monoacylglycerol acyltransferase from rat intestinal villus cells. Can. J. Biochem. Cell Biol. 63 (5), 341–347.

Manganaro, F., Kuksis, A., 1985b. Rapid isolation of a triacylglycerol synthetase complex from rat intestinal mucosa. Can. J. Biochem. Cell Biol. 63 (2), 107–114.

Marza, E., Barthe, C., Andre, M., Villeneuve, L., Helou, C., Babin, P.J., 2005. Developmental expression and nutritional regulation of a zebrafish gene homologous to mammalian microsomal triglyceride transfer protein large subunit. Dev. Dyn. 232 (2), 506–518.

McDonald, G.B., Saunders, D.R., Weidman, M., Fisher, L., 1980. Portal venous transport of long-chain fatty acids absorbed from rat intestine. Am. J. Physiol. 239 (3), G141–G150.

McKnight, S.L., 2010. On getting there from here. Science 330 (6009), 1338–1339.

Moore, T., 1982. Phsopholipid biosynthesis. Ann. Rev. Plant Physiol. 33, 235–259.

Morgan, T.H., 1932. The rise of genetics. Ii. Science 76 (1970), 285–288.

Nusslein-Volhard, C., 1994. Of flies and fishes. Science 266 (5185), 572–574.

Oka, T., Nishimura, Y., Zang, L., Hirano, M., Shimada, Y., Wang, Z., Umemoto, N., Kuroyanagi, J., Nishimura, N., Tanaka, T., 2010. Diet-induced obesity in zebrafish shares common pathophysiological pathways with mammalian obesity. BMC Physiol. 10, 21.

Pack, M., Solnica-Krezel, L., Malicki, J., Neuhauss, S.C., Schier, A.F., Stemple, D.L., Driever, W., Fishman, M.C., 1996. Mutations affecting development of zebrafish digestive organs. Development 123, 321–328.

Pagano, R.E., Martin, O.C., Kang, H.C., Haugland, R.P., 1991. A novel fluorescent ceramide analogue for studying membrane traffic in animal cells: accumulation at the Golgi apparatus results in altered spectral properties of the sphingolipid precursor. J. Cell Biol. 113 (6), 1267–1279.

Papamandjaris, A.A., MacDougall, D.E., Jones, P.J., 1998. Medium chain fatty acid metabolism and energy expenditure: obesity treatment implications. Life Sci. 62 (14), 1203–1215.

Sarda, L., Desnuelle, P., 1958. Actions of pancreatic lipase on esters in emulsions. Biochim. Biophys. Acta 30 (3), 513–521.

Schlegel, A., Stainier, D.Y., 2006. Microsomal triglyceride transfer protein is required for yolk lipid utilization and absorption of dietary lipids in zebrafish larvae. Biochemistry 45 (51), 15179–15187.

Schultz, C., Neef, A. B., Gadella, T. W., Jr. and Goedhart, J. (2010) 'Imaging lipids in living cells', Cold Spring Harb Protoc 2010(8): pdb top83.

Spandl, J., White, D.J., Peychl, J., Thiele, C., 2009. Live cell multicolor imaging of lipid droplets with a new dye, LD540. Traffic 10 (11), 1579–1584.

Stahl, A., Hirsch, D.J., Gimeno, R.E., Punreddy, S., Ge, P., Watson, N., Patel, S., Kotler, M., Raimondi, A., Tartaglia, L.A., et al., 1999. Identification of the major intestinal fatty acid transport protein. Mol. Cell. 4 (3), 299–308.

Steinberg, S.J., Wang, S.J., Kim, D.G., Mihalik, S.J., Watkins, P.A., 1999. Human very-long-chain acyl-CoA synthetase: cloning, topography, and relevance to branched-chain fatty acid metabolism. Biochem. Biophys. Res. Commun. 257 (2), 615–621.

Stoletov, K., Fang, L., Choi, S.H., Hartvigsen, K., Hansen, L.F., Hall, C., Pattison, J., Juliano, J., Miller, E.R., Almazan, F., et al., 2009. Vascular lipid accumulation, lipoprotein oxidation, and macrophage lipid uptake in hypercholesterolemic zebrafish. Circ. Res. 104 (8), 952–960.

Thomson, A.B., Keelan, M., Cheng, T., Clandinin, M.T., 1993. Delayed effects of early nutrition with cholesterol plus saturated or polyunsaturated fatty acids on intestinal morphology and transport function in the rat. Biochim. Biophys. Acta 1170 (1), 80–91.

Thumser, A.E., Storch, J., 2007. Characterization of a BODIPY-labeled fluorescent fatty acid analogue. Binding to fatty acid-binding proteins, intracellular localization, and metabolism. Mol. Cell. Biochem. 299 (1–2), 67–73.

Treibs, A., Kreuzer, F., 1969. Difluorboryl-Komplexe von Di- und Tripyrrylmethenen. Justus Liebigs Ann. Chem. 721, 116–120.

Vallot, A., Bernard, A., Carlier, H., 1985. Influence of the diet on the portal and lymph transport of decanoic acid in rats. Simultaneous study of its mucosal catabolism. Comp. Biochem. Physiol. A Comp. Physiol. 82 (3), 693–699.

van Greevenbroek, M.M., Voorhout, W.F., Erkelens, D.W., van Meer, G., de Bruin, T.W., 1995. Palmitic acid and linoleic acid metabolism in Caco-2 cells: different triglyceride synthesis and lipoprotein secretion. J. Lipid Res. 36 (1), 13–24.

Wallace, K., Pack, M., 2003. Unique and conserved aspects of gut development in zebrafish. Dev. Biol. 255 (1), 12–29.

Wallace, K.N., Akhter, S., Smith, E.M., Lorent, K., Pack, M., 2005. Intestinal growth and differentiation in zebrafish. Mech. Dev. 122 (2), 157–173.

Young, S.C., Hui, D.Y., 1999. Pancreatic lipase/colipase-mediated triacylglycerol hydrolysis is required for cholesterol transport from lipid emulsions to intestinal cells. Biochem. J. 339 (Pt 3), 615–620.

Yu, C., Xiao, W., Zhang, D., Ou, W., Feng, Z. and Zhu, W. (2010) 'Study on characterization of the complexes of FUS1/hIL-12 with cationic liposome', 27(4): 859–64.

Zhang, S.O., Trimble, R., Guo, F., Mak, H.Y., 2010. Lipid droplets as ubiquitous fat storage organelles in C. elegans. BMC Cell Biol. 11, 96.